Langmuir

Article

pubs.acs.org/Langmuir

Direct Intercalation of Bis-2,2′,2″,6-terpyridylcobalt(III) into Zirconium Phosphate Layers for Biosensing Applications

Mitk'El B. Santiago-Berríos,[†] Chasterie Declet-Flores,[‡] Amanda David,[‡] Solmarie Borrero,[‡] Meredith M. Vélez,[‡] Agustín Díaz-Díaz,[‡] Ana R. Guadalupe,[‡] and Jorge L. Colón*[,‡]

[†]School of Science and Technology, Universidad Metropolitana, Apartado 21150, San Juan, Puerto Rico (PR) 00928-1150, Puerto Rico

[‡]Department of Chemistry, University of Puerto Rico, Río Piedras Campus, Post Office Box 23346, San Juan, Puerto Rico (PR) 00931-3346, Puerto Rico

Supporting Information

ABSTRACT: The direct intercalation reaction of $[Co(tpy)_2]^{2+}$ with the highly hydrated θ phase of layered zirconium phosphate (θ-ZrP) resulted in the formation of the oxidized $[Co(tpy)_2]^{3+}$ ion within the ZrP material. The X-ray powder diffraction patterns showed that the interlayer distance increases from 10.3 Å in θ-ZrP to 14.9 Å in the dry $[Co(tpy)_2]^{3+}$-intercalated ZrP {$[Co(tpy)_2]^{3+}$:ZrP} phase. The complex remains electroactive within the layers of ZrP. The formal potential of a carbon paste electrode (CPE) modified with $[Co(tpy)_2]^{3+}$:ZrP ($E^{\circ\prime}$ = 40.8 mV versus Ag/AgCl, 3.5 M NaCl) is non-pH-dependent. However, the sensitivity of the $[Co(tpy)_2]^{3+}$:ZrP-modified CPE for the detection of reduced nicotinamide adenine dinucleotide (NADH) electrooxidation was lower than that of a previously reported CPE modified with $[Ru(phend)_2bpy]^{2+}$-intercalated ZrP.[1] To improve the characteristics of NADH electrooxidation of the $[Co(tpy)_2]^{3+}$:ZrP-modified CPE, we included the enzyme diaphorase in solution, which increased the electrocatalytic current for NADH oxidation. A bienzymatic lactate biosensor was constructed and used for lactate sensing.

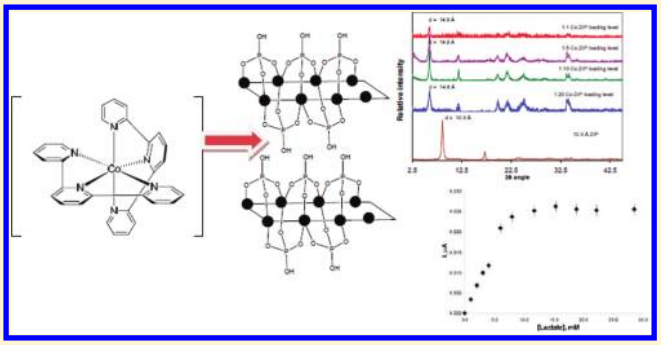

INTRODUCTION

The development of biosensor and bioelectronic devices commonly requires the integration of the biomaterial (e.g., an enzyme) with an electron mediator that enables electronic amplification of the biorecognition or biocatalytic events occurring on the transducer. Good mediators should (a) be sufficiently small to be able to reach usually buried enzyme active sites, (b) have an appropriate redox potential ($E^{\circ\prime}$), (c) have a high electron exchange rate between oxidized or reduced enzyme active sites, and (d) have a medium-independent Nerstian electrode behavior.[2−5] The self-exchange rate is known to be higher for complexes with a rigid ligand shell, which minimizes the reorganization energy in the redox process.[2−5]

The possible redox mediators for reduced nicotinamide adenine dinucleotide (NADH) oxidation are of two types: one-electron/non-proton and two-electron/one- or two-proton acceptors/donors. One-electron/non-proton mediators have the advantage that protons do not participate in their redox conversion ($E^{\circ\prime}$ constant with changes in pH) and no radical intermediates promote side reactions. However, studies have shown that two-electron/one-proton acceptors are better oxidants than one-electron/non-proton acceptors for NADH oxidation.[4−10]

When the electron mediator is immobilized on the electrode surface, the NADH oxidation can be analyzed using a Michaelis−Menten-like mechanism.[2] The electrochemical reaction is heterogeneous, although the electron transfer (ET) must occur when the activated complex is formed. Typical second-order rate constant values are below 10^4 M^{-1} s^{-1}; very few mediators have second-order rate constants in the range from 10^4 to 10^6 M^{-1} s^{-1}.[4] These values suggest that the ET mechanism is mass-transfer-controlled. Several mediators have shown large second-order rate constants but have required large overpotentials.[2] Many attempts have been performed to build more efficient amperometric NAD^+/NADH biosensors that exhibit large second-order rate constants, including preparing self-contained sensors.[11,12]

Guadalupe et al. and Abruña et al. have used $[Co(tpy)_2]^{2+}$ and its derivatives to detect the electrooxidation of NADH in solution.[13,14] Guadalupe et al. also used $[Co(tpy)_2]^{2+}$ for lactate sensing using lactate dehydrogenase in a monoenzymatic setup and lipoamide dehydrogenase and lactate dehydrogenase in a bienzymatic setup.[13]

Received: September 7, 2011
Revised: February 3, 2012
Published: February 8, 2012

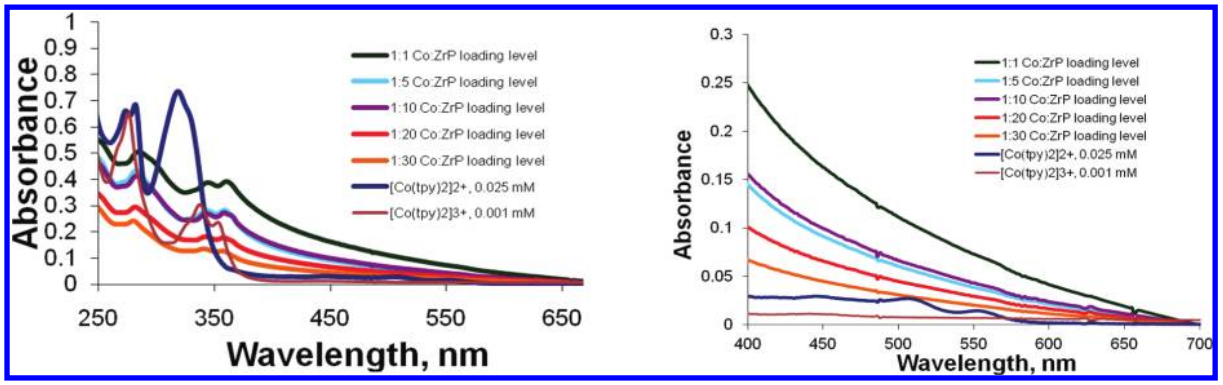

Figure 1. (a) UV−vis absorption spectra of a 0.025 mM $[Co(tpy)_2]^{2+}$ aqueous solution, a 0.001 mM $[Co(tpy)_2]^{3+}$ aqueous solution, and the various Co:ZrP loading levels. (b) MLCT UV−vis absorption spectra region using the same concentrations as in panel a.

The goal of finding materials that can improve the stability of self-contained biosensors is a priority. Zirconium phosphate (ZrP) layers are an attractive alternative and have attracted attention in recent studies.[15−17] ZrPs are layered ion-exchange materials; the α phase of ZrP has been widely characterized and studied.[18−26] Marti and Colón reported the immobilization, without any pre-intercalation step, of tris(2,2′-bipyridine)-ruthenium(II) $[Ru(bpy)_3^{2+}]$ into an hydrated form of ZrP known as the 10.3 Å phase (10.3 Å-ZrP or θ-ZrP).[27] Several inorganic and organic compounds have been immobilized using this method.[28−30] We recently reported the direct intercalation of bis(1,10-phenanthroline-5,6-dione)(2,2′-bipyridine)-ruthenium(II) $\{[Ru(phend)_2]^{2+}\}$ into ZrP.[1,31] A carbon paste electrode (CPE) modified with the $[Ru(phend)_2]^{2+}$-intercalated ZrP material showed catalytic behavior toward NADH oxidation, and an ethanol sensor was developed.

We report here that the direct intercalation reaction of $[Co(tpy)_2]^{2+}$ with θ-ZrP produces $[Co(tpy)_2]^{3+}$-intercalated ZrP $\{[Co(tpy)_2]^{3+}$:ZrP$\}$. These materials have been prepared to construct a lactate sensor, in which the electron mediator can oxidize NADH but whose electrochemical behavior is not pH-dependent. Cobalt complexes have been used for NADH oxidation.[13,14,32] We present in this paper the electrode kinetics of a CPE modified with $[Co(tpy)_2]^{3+}$:ZrP in the presence of NADH. A bienzymatic lactate sensor based on the $[Co(tpy)_2]^{3+}$:ZrP-modified CPE is also described.

RESULTS AND DISCUSSION

Intercalation and Spectroscopical Characterization of $[Co(tpy)_2]^{3+}$-Exchanged ZrP Materials. Experimental details appear in the Supporting Information. Samples of $[Co(tpy)_2]^{3+}$-exchanged ZrP were prepared from suspensions of ZrP at different $[Co(tpy)_2](PF_6)_2$ concentrations. The intercalation products were filtered and allowed to dry overnight. To determine if the complex had undergone a chemical reaction during the intercalation process, ultraviolet−visible (UV−vis) spectrophotometry and Fourier transform infrared (FTIR) spectroscopy measurements were performed.

Figure 1 shows the UV−vis absorbance spectra of a 0.025 mM $[Co(tpy)_2]^{2+}$ aqueous solution, a 0.001 mM $[Co(tpy)_2]^{3+}$ aqueous solution, and the 0.008% (m/v) suspensions of the Co:ZrP materials at various loading levels. The absorbance increases with an increase in the loading level. Figure 1 shows that the absorbance spectra of the immobilized complex are somewhat different from that of the complex in solution. The absorbance spectrum of the 0.025 mM $[Co(tpy)_2]^{2+}$ aqueous solution has three bands at 275, 280, and 320 nm, a shoulder at 328 nm corresponding to the $\pi-\pi^*$ transitions, and two small MLCT transitions at 500 and 550 nm.[33,34] Upon oxidation of $[Co(tpy)_2]^{2+}$ to $[Co(tpy)_2]^{3+}$, these metal-to-ligand charge-transfer (MLCT) transition bands disappear and the $\pi-\pi^*$ transition bands shift to 276, 339, and 354 nm, as observed in Figure 1 for a 0.001 mM $[Co(tpy)_2]^{3+}$ aqueous solution. The absorbance bands observed in Figure 1 for the intercalated complex are red-shifted to 286, 346, and 362 nm compared to those of Co^{2+} and Co^{3+} aqueous solutions. The spectra observed for the intercatated materials are more consistent (although red-shifted) with the presence of the oxidized complex in the intercalated material.[34]

Figure 2 shows the infrared (IR) spectra of $[Co(tpy)_2](PF_6)_2$ and the $[Co(tpy)_2]^{3+}$-intercalated ZrP materials at various

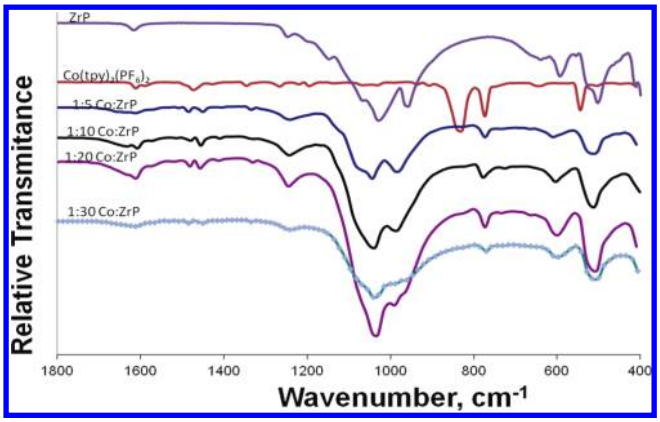

Figure 2. IR spectra of ZrP, $[Co(tpy)_2](PF_6)_2$, and $[Co(tpy)_2]^{3+}$-exchanged ZrP material at various loading levels.

loading levels. The ZrP lattice water bands that appear at 3580 and 3494 cm^{-1} diminish upon intercalation of $[Co(tpy)_2]^{3+}$ because of water displacement from the ZrP lattice, in agreement with previous results (data not shown).[35] The other ZrP lattice water vibrational band at 1610 cm^{-1} does not diminish in intensity because $[Co(tpy)_2](PF_6)_2$ also has a vibrational band at that wavenumber. In addition, Co:ZrP shows two additional vibrational bands at 1474 and 1439 cm^{-1}. These bands are also consistent with the formation of $[Co(tpy)_2]^{3+}$ species inside the ZrP matrix, confirming the UV−vis spectrophotometric results. These results suggest the intercalation of $[Co(tpy)_2]^{3+}$ into the layers of ZrP.

To verify if $[Co(tpy)_2]^{3+}$ was intercalated inside ZrP or mainly surface-bound, we performed X-ray powder diffraction

dx.doi.org/10.1021/la2035104 | Langmuir 2012, 28, 4447−4452

(XRPD) measurements. Figure 3 shows the characteristic XRPD patterns at different Co:ZrP loading levels. As the

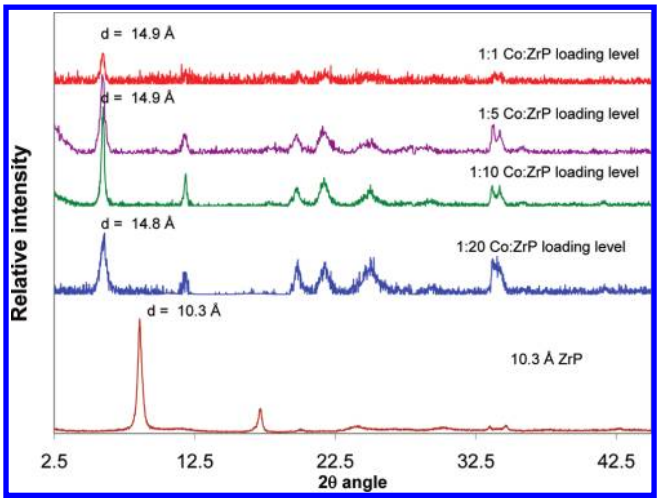

Figure 3. XRPD patterns for the $[Co(tpy)_2]^{3+}$-exchanged ZrP materials at various loading levels and the 10.3 Å phase of ZrP.

loading level is increased, the formation of a new phase with an expanded 14.9 Å interlayer distance is observed, indicating that $[Co(tpy)_2]^{3+}$ was intercalated into the ZrP layers. Using the dimensions of $[Co(tpy)_2]^{3+}$ (10.0 × 13.1 × 12.5 Å, calculated using Spartan), the minimum distance that $[Co(tpy)_2]^{2+}$ can separate the ZrP layers is by 10.0 Å. The thickness of a ZrP sheet as discussed before is 6.6 Å;[36] adding the expansion produced by $[Co(tpy)_2]^{3+}$ ions, the expected interlayer distance for the $[Co(tpy)_2]^{3+}$-intercalated ZrP material would be 16.6 Å. There is a difference of 1.7 Å between the calculated and observed Co:ZrP interlayer distance. However, as observed with $[Ru(phend)_2bpy]^{2+}$, a slight penetration between the phosphate groups can contribute to the reduced observed interlayer distance.[1]

Construction and Electrochemical Characterization of CPEs Modified with $[Co(tpy)_2]^{3+}$:ZrP. Figure 4 shows

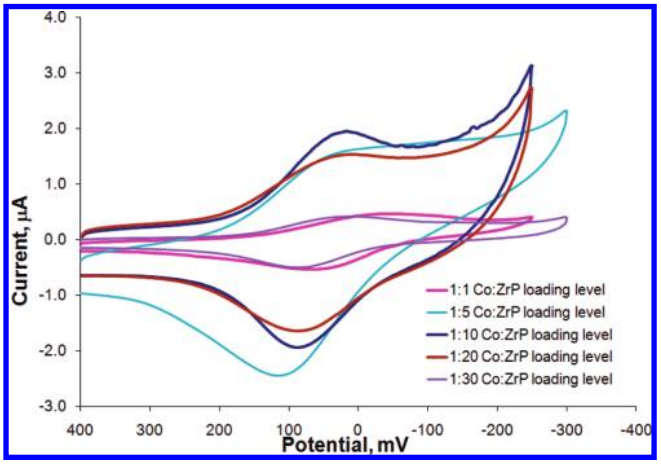

Figure 4. Cyclic voltammograms of modified CPEs at different Co:ZrP loading levels, in phosphate-buffered saline (PBS), 0.1 M at pH 7.0 (scan rate = 100 mV/s).

characteristic cyclic voltammograms of the CPEs modified with $[Co(tpy)_2]^{3+}$:ZrP, which confirm that the complex remains electroactive within ZrP. We observe a formal potential of 40.8 mV versus Ag/AgCl, which is in agreement with literature values for this complex.[13] Table 1 shows the

Table 1. Electrochemical Parameters of the Modified CPEs with Co:ZrP at Different Loading Levels (in PBS, 0.1 M at pH 7.0, with a Scan Rate = 100 mV/s)

Co:ZrP molar ratios	$E^{\circ\prime}$ (mV)	ΔE_p (mV)	i_{pa}/i_{pc}
1:1	34.0	59.0	1.00
1:5	40.8	61.0	1.01
1:10	39.0	33.8	1.19
1:20	38.8	29.0	1.13
1:30	43.5	60.5	1.01

electrochemical parameters of these modified CPEs. Although we observed that the complex remains electroactive, we cannot explain the erratic behavior in the different loading levels. However, we used the 1:5 loading level for further experiments because it has a higher concentration of the cobalt complex.

Figure 5 shows the Randles–Sevcik plot and its logarithm plot for the 1:5 Co:ZrP-modified CPE. The linear behavior observed in Figure 5a suggests that electron transfer on the electrode surface is mainly diffusion-controlled. However, because the slope of the logarithm plot in Figure 5b is different from 0.5, it shows that the electron transfer also has a nondiffusional component, as previously observed for the $[Ru(phend)_2bpy]^{2+}$-intercalated ZrP-modified CPE.[1] Because the electrodes showed no leaching (as evidenced by UV–vis spectrophotometry), the diffusional component corresponds to charge transport assisted by counterion diffusion, as observed previously for other intercalated ZrP-modified CPEs. In the case of $[Ru(phend)_2bpy]^{2+}$, we observed that, upon increasing the concentration of the complex inside the ZrP matrix, electrochemical reversibility was observed.[1] Although counterion diffusion is observed in these types of processes, it is probable that the redox species also couple electronically by electron-hopping mechanisms. Electron hopping occurs by "electron self-exchange", where a reduced species simply transfers electrons to their oxidized counterpart of the same species.[37]

Electrocatalysis of NADH by CPEs Modified with $[Co(tpy)_2]^{3+}$:ZrP. We performed experiments to determine if this complex intercalated into ZrP can be used for NADH electrooxidation (further experiments were performed using the 1:5 Co:ZrP-modified CPE because it demonstrated better electrochemical and chemical reversibility). Figure 6 shows cyclic voltammograms of CPE modified with $[Co(tpy)_2]^{3+}$:ZrP in the absence and presence of NADH. When a known concentration of NADH is added to the elecrtrolytic cell, a catalytic current is observed. Figure 6 shows that the onset of the catalytic current began at 0 mV and reaches a catalytic current at ca. 45 mV.

We constructed carbon paste rotating disk electrodes modified with the 1:5 $[Co(tpy)_2]^{3+}$:ZrP material to construct a calibration plot for the NADH concentration. Figure 7 shows a characteristic calibration plot for NADH oxidation using this modified carbon paste rotating disk electrode. The shape of the calibration plot suggests a Michaelis–Menten-like mechanism.[1,38] To further evaluate a Michaelis–Menten mechanism, we plotted the reciprocal plot of the current and NADH concentration (see inset) of the linear plot of the calibration plot. By solving eq 4 (see the Supporting Information for more details), the K_M of the electrochemical process was evaluated to

dx.doi.org/10.1021/la2035104 | Langmuir 2012, 28, 4447–4452

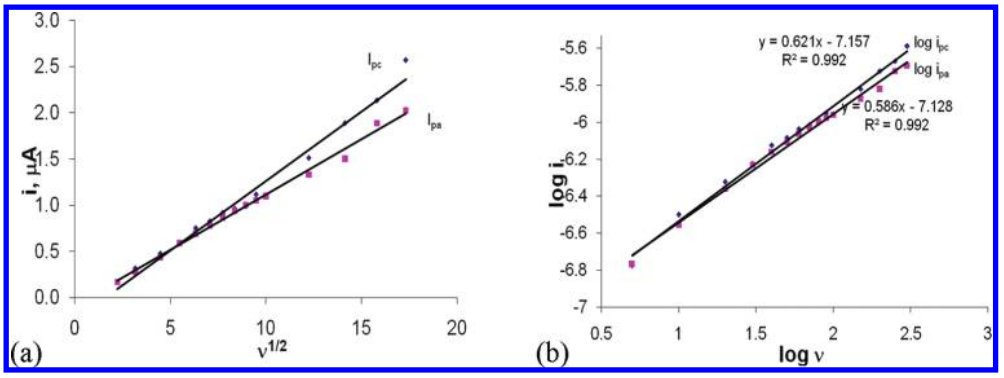

Figure 5. (a) Randles–Sevcik plot for the 1:5 Co:ZrP-modified CPE. (b) Logarithm plot of the data plotted in panel a.

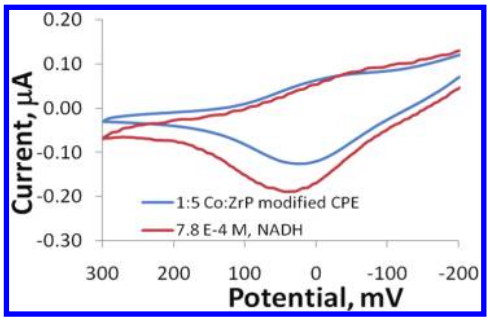

Figure 6. Steady-state cyclic voltammograms at 5 mV/s of Co:ZrP-modified CPE in the absence and presence of NADH in PBS (0.1 M at pH 7.0).

be 0.004 mM and the k_{+2} value was 0.52 s^{-1}; both values are smaller in comparison to the values obtained with the $[Ru(phend)_2bpy]^{2+}$:ZrP material (K_M = 5.27 mM, and k_{+2} = 1068.37 s^{-1}).[1] The smaller value obtained for $[Co(tpy)_2]^{3+}$:ZrP is probably due to the activation complex in the electrode surface not being as stable, and the electron-transfer process is not centered in the ligand but, instead, occurs at the metal center. In contrast, for the $[Ru(phend)_2bpy]^{2+}$ mediator, the electrochemistry responsible for NADH oxidation is centered on the phendione ligand, which is more accessible to react with NADH.

To determine the second-order rate constant k_{obs}, the Koutecky–Levich equation must be used. Figure 7b shows the Koutecky–Levich plot for the determination of k_{obs} at various rotation frequencies for the 1:5 $[Co(tpy)_2]^{3+}$:ZrP loading level. The k_{obs} value obtained, 3.61 × 10^5 M^{-1} s^{-1}, is higher than that observed for CPE modified with $[Ru(phend)_2bpy]^{2+}$-intercalated ZrP (1.24 × 10^5 M^{-1} s^{-1} at pH 7.0).[1] The higher k_{obs} value for $[Co(tpy)_2]^{3+}$:ZrP-modified CPE is expected because the applied potential (45 mV) allows for greater electromotive force for NADH oxidation and also the onset for NADH oxidation begins at 50 mV.[5,39]

Lactate Sensing with CPE Modified with Co:ZrP. Guadalupe et al. used $[Co(tpy)_2]^{2+}$ for lactate sensing[13] and demonstrated that coupling it to lipoamide dehydrogenase (LADH) or diaphorase can increase the catalytic current for NADH oxidation. The construction of bienzymatic devices by coupling mediators allows for a decrease in the overpotential for NADH electrooxidation and avoidance of common interferences for electrode fouling.[40−44] LADH or diaphorase allows for the complete NADH oxidation to form NAD^+ that can be reused in the catalytic cycle, without forming any radicals on the electrode surface.

Diaphorase has two flavin adenine molecules bound in the active site but no metal ion.[40] The two flavins are capable of shuttling electrons to an electron acceptor. Diaphorase has also been called NADH dehydrogenase and NADH-acceptor oxidoreductase.[41,43] The diaphorase has been used as an electron shuttle, reducing electron fouling, and by coupling with another enzyme, it can be used for the detection of numerous substrates. The result of coupling diaphorase with another enzyme is to increase the current density in the presence of the substrate of interest.

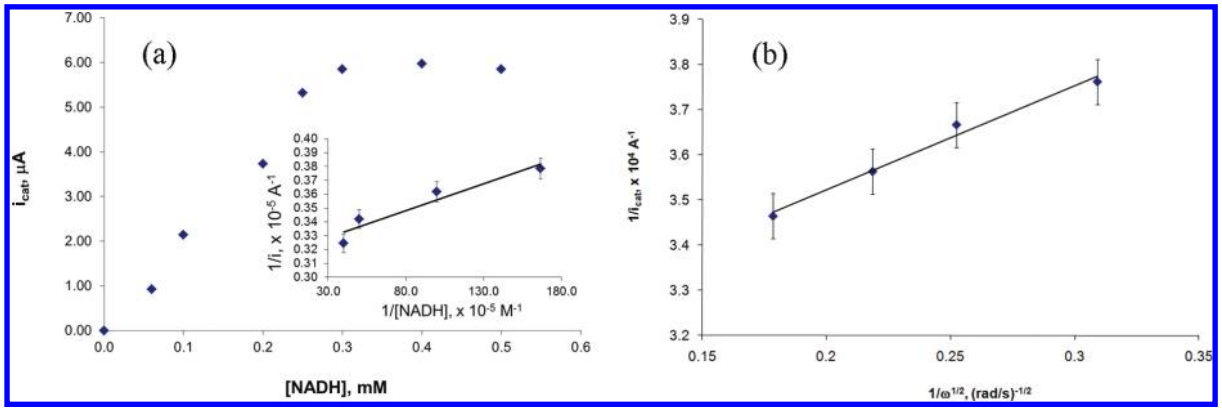

Figure 7. (a) Calibration plot for NADH electrooxidation using a $[Co(tpy)_2]^{3+}$:ZrP-modified rotating CPE at 100 rpm, in PBS, 1 M at pH 7.0. (Inset) Reciprocal plot of the current as a function of the concentration. (b) Variation of $1/i_{cat}$ as a function of $1/\omega^{1/2}$ for the determination of k_{obs} with the 1:5 Co:ZrP-modified rotating CPE at pH 7.0 (PBS, 0.1 M; [NADH] = 0.01 mM; scan rate = 5.0 mV/s).

dx.doi.org/10.1021/la2035104 | *Langmuir* 2012, 28, 4447−4452

We performed an analogous experiment where we compared the electrocatalytic current for the electrooxidation of NADH in the absence and presence of diaphorase using the $[Co(tpy)_2]^{3+}$:ZrP-modified CPE. Figure 8 shows the calibration

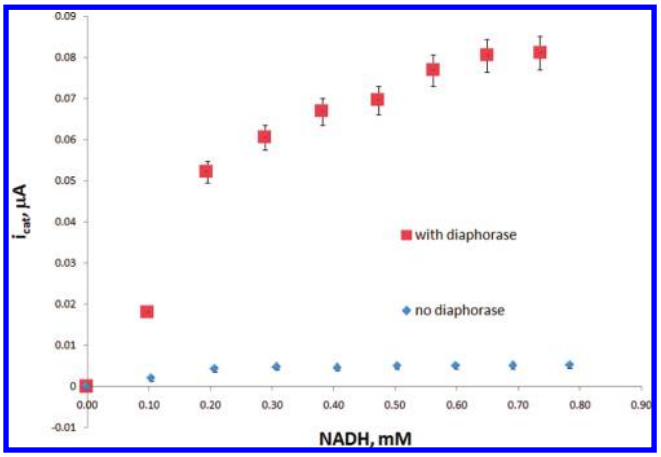

Figure 8. Calibration plot for NADH oxidation by $[Co(tpy)_2]^{3+}$:ZrP-modified CPE in the absence and presence of diaphorase (7.6 units/mL; PBS, 0.1 M at pH 7.0).

plot for NADH oxidation in the presence and absence of diaphorase (see also Figure 3S in the Supporting Information). We observed that, in the presence of diaphorase, the electrooxidation of NADH is enhanced and the catalytic current can be differentiated. The difference in the catalytic current can be attributed to the use of the $FADH_2$-bound diaphorase. Figure 8 shows that the electrocatalytic current is enhanced by ca. 10-fold in the presence of diaphorase. It is known that $FADH_2$ is a better electron shuttle than NADH alone.[13] Similar experiments were performed with CPEs modified with $[Co(tpy)_2]^{2+}$ by Guadalupe et al., where in the presence of diaphorase, the electrocatalytic current was also enhanced.[13] The authors attributed that this change in electrocatalytic current is due to the fact that $[Co(tpy)_2]^{2+}$ can enter the enzyme active site and shuttle the electrons to the electrode surface.

To compare a monoenzymatic system with a bienzymatic system, we constructed a bienzymatic lactate sensor as demonstrated in Scheme 1. When lactate dehydrogenase

Scheme 1. Bienzymatic Scheme for Lactate Sensing

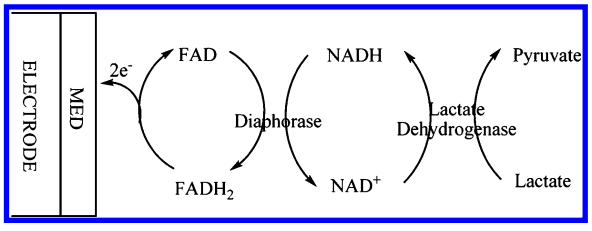

oxidizes lactate to form pyruvate, NADH is formed. NADH is then oxidized in the presence of a diaphorase to form $FADH_2$. $FADH_2$ then transfers its electrons to the electrode surface. Therefore, we can use this scheme to determine the lactate concentration in the presence of these two enzymes. In our setup, the mediator layer in the surface is the $[Co(tpy)_2]^{3+}$:ZrP material.

We performed experiments where we coupled lactate dehydrogenase with diaphorase to determine the lactate concentration using Co:ZrP-modified CPE. Similar experiments where performed by Colón and Guadalupe for $[Co(tpy)_2]^{2+}$ in solution and in $[Co(tpy)_2]^{2+}$-modified CPEs.[13] We performed experiments in the presence of diaphorase, NAD^+, and lactate dehydrogenase. Figure 9

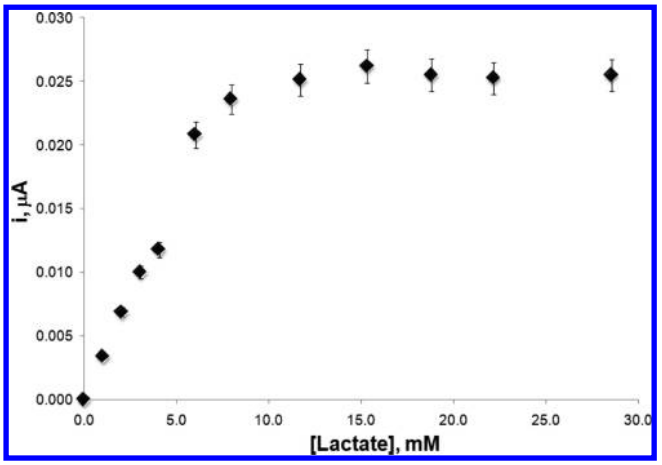

Figure 9. Calibration plot for lactate sensing using $[Co(tpy)_2]^{3+}$:ZrP-modified CPE in the presence of 20 units/mL lactate dehydrogenase, diaphorase, and 20 mM NAD^+ in PBS, 0.1 M at pH 7.0, at 5 mV/s.

shows the steady-state catalytic response of the $[Co(tpy)_2]^{3+}$:ZrP-modified CPE at various lactate concentrations. When no lactate is added to the electrochemical cell, no electrocatalytic current was observed. Once lactate is present at the electrochemical cell, an electrocatalytic current is observed. We found a linear behavior up to 10 mM, where saturation occurs at the electrode surface. This behavior is expected for a Michaelis–Menten-like mechanism.

Colón and Guadalupe also constructed a bienzymatic lactate sensor and obtained a linear range up to 5 mM in the same experimental conditions, except with no ZrP.[13] The linear range of their sensor is smaller in comparison to ours, where the linear range reaches up to 10 mM. The sensitivity of their approach reaches to 0.48 μA/[lactate, mM]. Our method has a sensitivity of 0.003 μA/[lactate, mM]. This result is an advantage because lactate concentrations in blood and cerebrospinal fluid are below 4 mM.[13] In addition, sensitivity in clinical samples is very important to diagnose diseases. Therefore, these concentrations can easily be determined with our modified CPE.

In conclusion, we have immobilized $[Co(tpy)_2]^{3+}$ inside the layers of ZrP by reacting $[Co(tpy)_2](PF_6)_2$ with the 10.3 Å ZrP phase. The acidic environment oxidized the cobalt ion was demonstrated by UV–vis and FTIR spectrophotometry. Modified CPEs were constructed, and these materials remain chemically and electrochemically stable upon intercalation. The formal potential is not pH-dependent, in agreement with previous reports.[13,14]

The modified CPEs were then analyzed in the presence of NADH. The electron transfer for the process of NADH oxidation follows a Michaelis–Menten mechanism. To increase the NADH oxidation signal, we put the modified CPE in the presence of diaphorase. The electrocatalytic current for the NADH oxidation was enhanced 10-fold, showing that the flavin center of the diaphorase is a better electron shuttle than

dx.doi.org/10.1021/la2035104 | Langmuir 2012, 28, 4447–4452

NADH. We constructed a bienzymatic lactate sensor and detected lactate concentrations up to 10 mM. These findings help us to better design ZrP materials as matrices for the immobilization of electron shuttles for the construction of amperometric biosensors.

■ ASSOCIATED CONTENT

Supporting Information

Synthesis of $[Co(tpy)_2](PF_6)_2$, intercalation reaction of $[Co(tpy)_2]^{2+}$ with ZrP, modified CPE preparation, kinetic studies for the electrooxidation of NADH for the Co:ZrP-modified CPEs, theoretical calculations of $[Co(tpy)_2]^{2+}$ into zirconium phosphates, XPS studies, electrochemical studies at different pH values, and NADH electrochemical response in the presence and absence of diaphorase. This material is available free of charge via the Internet at http://pubs.acs.org.

■ AUTHOR INFORMATION

Corresponding Author

*E-mail: jorge.colon10@upr.edu.

Notes

The authors declare no competing financial interest.

■ REFERENCES

(1) Santiago, M. B.; Vélez, M. M.; Borrero, S.; Díaz, A.; Casillas, C. A.; Hofmann, C.; Guadalupe, A. R.; Colón, J. L. *Electroanalysis* **2006**, *18*, 559−572.

(2) Lobo, M. J.; Miranda, A. J.; Tuñón, P. *Electroanalysis* **1997**, *9*, 191−202.

(3) Gorton, L. *J. Chem. Soc., Faraday Trans. 1* **1986**, *82*, 1245−1258.

(4) Gorton, L.; Domínguez, E. In *Encyclopedia of Electrochemistry*; Bard, A. J., Stratmann, M., Wilson, G. S., Eds.; Wiley-VCH, GmbH: Weinheim, Germany, 2002; Vol. *9*.

(5) Gorton, L.; Domínguez, E. *Rev. Mol. Biotechnol.* **2002**, *82*, 371−392.

(6) Kitani, A.; Miller, L. L. *J. Am. Chem. Soc.* **1981**, *103*, 3595−3597.

(7) Kitani, A.; So, Y.-H.; Miller, L. L. *J. Am. Chem. Soc.* **1981**, *103*, 7636−7641.

(8) Carlson, B. W.; Miller, L. L. *J. Am. Chem. Soc.* **1983**, *105*, 7453−7454.

(9) Carlson, B. W.; Miller, L. L.; Neta, P.; Grodkowski, J. *J. Am. Chem. Soc.* **1984**, *106*, 7233−7239.

(10) Carlson, B. W.; Miller, L. L. *J. Am. Chem. Soc.* **1985**, *175*, 479−485.

(11) Armstrong, F. A.; Wilson, G. S. *Electrochim. Acta* **2000**, *45*, 2623−2645.

(12) Burgess, J. D.; Hawkridge, F. M. In *Electroanalytical Methods for Biological Material*; Brajter-Toth, A., Chambers, J. Q., Eds.; Marcel Dekker: New York, 2002.

(13) Colón, C. M.; Guadalupe, A. R. *Electroanalysis* **1998**, *10*, 621−627.

(14) Storrier, G. D.; Takada, K.; Abruña, H. D. *Inorg. Chem.* **1999**, *38*, 559−565.

(15) Alberti, G. *Acc. Chem. Res.* **1978**, *11*, 163−170.

(16) Clearfield, A. *Chem. Rev.* **1988**, *88*, 125−148.

(17) Clearfield, A. *Prog. Inorg. Chem.* **1998**, *47*, 371−509.

(18) Clearfield, A. *Curr. Opin. Solid State Mater. Sci.* **2002**, *6*, 485−506.

(19) Sue, H. J.; Gam, K. T.; Bestaoui, N.; Spurr, N.; Clearfield, A. *Chem. Mater.* **2004**, *16*, 242−249.

(20) Sun, L.; Boo, W. J.; Browning, R. L.; Sue, H. J.; Clearfield, A. *Chem. Mater.* **2005**, *17*, 5606−5609.

(21) Takei, T.; Kobayashi, Y.; Hata, H.; Yonesaki, Y.; Kumada, N.; Kinomura, N.; Mallouk, T. E. *J. Am. Chem. Soc.* **2006**, *128*, 16634−16640.

(22) Bestaoui, N.; Spurr, N.; Clearfield, A. *J. Mater. Chem.* **2006**, *16*, 759−764.

(23) Sun, L.; Boo, W. J.; Sue, H. J.; Clearfield, A. *New J. Chem.* **2007**, 39−43.

(24) Shi, S.; Zhou, J.; Zong, R.; Te, J. *J. Lumin.* **2007**, *122*−*123*, 218−220.

(25) Ferragina, C.; Di Rocco, R.; Giannoccaro, P.; Parono, P.; Petrilli, L. *J. Inclusion Phenom. Macrocyclic Chem.* **2009**, *63*, 1−9.

(26) Ferragina, C.; Di Rocco, R.; Giannoccaro, P.; Petrilli, L. *Mater. Res. Bull.* **2010**, *45*, 34−39.

(27) Martí, A. A.; Colón, J. L. *Inorg. Chem.* **2003**, *42*, 2830−2832.

(28) Martí, A. A.; Paralitici, G.; Maldonado, L.; Colón, J. L. *Inorg. Chim. Acta* **2006**, *360*, 1535−1542.

(29) Bermúdez, R. A.; Colón, Y.; Tejada, G. A.; Colón, J. L. *Langmuir* **2005**, *21*, 890−895.

(30) Rivera, E. J.; Figueroa, C.; Colón, J. L.; Grove, L.; Connick, W. B. *Inorg. Chem.* **2007**, *46*, 8569−8576.

(31) Santiago, M. B.; Daniel, G. A.; David, A.; Casañas, B.; Hernández, G.; Guadalupe, A. R.; Colón, J. L. *Electroanalysis* **2010**, *22*, 1097−1105.

(32) Guadalupe, A. R.; Usifer, D. A.; Potts, K. T.; Hurrell, H. C.; Mogstad, A.-E.; Abruña, H. D. *J. Am. Chem. Soc.* **1988**, *110*, 3462−3466.

(33) Potts, K. T.; Usifer, D. A.; Guadalupe, A. R.; Abruña, H. D. *J. Am. Chem. Soc.* **1987**, *109*, 3961−3967.

(34) Vitello, L. B.; Erman, J. E. *J. Biol. Inorg. Chem.* **2001**, *6*, 578−589.

(35) Horsley, S. E.; Nowell, D. V.; Stewart, D. T. *Spectrochim. Acta* **1974**, *30A*, 535−541.

(36) Troup, J. M.; Clearfield, A. *Inorg. Chem.* **1977**, *16*, 3311−3314.

(37) Martin, C. R.; Foss, C. A. In *Laboratory Techniques in Electroanalytical Chemistry*; Kissinger, P. T., Heineman, W. R., Eds.; Marcel Dekker: New York, 1996.

(38) Lyons, M. E. G. *Sensors* **2002**, *2*, 473−506.

(39) Blankespoor, R. L.; Miller, L. L. *J. Electroanal. Chem.* **1984**, *171*, 231−241.

(40) Matsue, T.; Chang, H.-C.; Uchida, I.; Osa, T. *Tetrahedron Lett.* **1988**, *29*, 1551−1554.

(41) Matsue, T.; Yamada, H.; Chang, H.-C.; Uchida, I.; Nagata, K.; Tomita, K. *Biochim. Biophys. Acta* **1990**, *1038*, 29−38.

(42) Matsue, T.; Kasai, N.; Narumi, M.; Nishizawa, M.; Yamada, H.; Uchida, I. *J. Electroanal. Chem.* **1991**, *300*, 111−118.

(43) Chang, H.-C.; Ueno, K.; Yamada, H.; Matsue, T.; Uchida, I. *Analyst* **1991**, *116*, 793−796.

(44) Tatsuma, T.; Watanabe, T. *J. Electroanal. Chem.* **1991**, *310*, 149−157.